Dear Editor,

We are pleased to submit the revised version of our manuscript entitled “Estimation of Nocturnal Boundary Layer Height in the Central Amazon, Supported by Gas Concentration Profiles” by Souza et al. We sincerely thank the reviewers for their constructive comments and suggestions, which helped us substantially improve the manuscript.

We reorganized the overall structure of the manuscript to improve its clarity and readability. In particular, we separated the Results and Discussion sections, allowing the results to be presented more objectively and the physical interpretation of the findings to be developed in depth in a dedicated Discussion section.

In the revised version, we carefully addressed all reviewer comments and expanded the manuscript in several important aspects. In particular, following the suggestions of Reviewers 1 and 2, we extended the discussion of the physical drivers controlling the seasonal, interannual, and case-study variability of the nocturnal boundary-layer height (hn). We now provide a more detailed interpretation of the roles of nocturnal radiative cooling, atmospheric stability, cloud cover, vertical profile of the potential temperature gradients, and mechanically generated turbulence.

These additions allowed us to better quantify and interpret the mechanisms behind the contrasting hn behavior observed during the selected nights.

In addition, we expanded the discussion of how the Amazon forest canopy influences nocturnal stratification and vertical mixing. We now explicitly discuss the canopy as a roughness and drag layer that can enhance coupling or decoupling between the air near the forest top and the atmosphere above, depending on the balance between thermal stratification and shear-generated turbulence.

We further improved the interpretation of the CO and CH4 concentration profiles by considering background trace-gas concentrations during the days preceding the case-study nights, as well as the influence of wind direction, source regions, previous plume history, and hn variability. Additional supplementary analyses were included to support this interpretation, including multi-day CO and CH4 concentration time series and two additional nocturnal case studies.

Overall, the revision substantially broadened the scope and depth of the manuscript. What was initially a more focused analysis of nocturnal boundary-layer height supported by gas concentration profiles has now been expanded into a more complete study of the physical mechanisms controlling hn variability and its implications for trace-gas vertical exchange over the central Amazon forest. We believe that these changes make the manuscript more suitable as a full research article in Atmospheric Chemistry and Physics.

We thank you and the reviewers again for your time and valuable feedback. We hope that the revised manuscript is now suitable for publication in Atmospheric Chemistry and Physics.

Sincerely,

Cléo Quaresma Dias-Júnior
on behalf of all co-authors

Review of MS. MS No.: EGUSPHERE-2025-6531

Title: Estimation of nocturnal boundary layer height in the central Amazon, supported by gas concentration profiles

Response (blue color) to anonymous **Referee #1** (black). The original manuscript was changed accordingly.

General comments

This manuscript addresses a timely and potentially interesting topic of the dynamics of the nocturnal boundary layer and the impact on the gas concentration profiles in a remote location of the Amazonia. The meteorological and atmospheric composition data is very comprehensive. However, the analysis and interpretation remain largely descriptive and do not sufficiently engage with the underlying physical mechanisms or relevant observational and theoretical studies. Substantial additional work would be required to strengthen the physical interpretation of the dynamics of the Amazonian Nocturnal Boundary Layer (ANBL) and fully exploit the observations. Given the extent of revisions needed, we recommend rejection at this stage, with the encouragement that the authors resubmit a thoroughly revised manuscript after deeper physical and observational analysis. In the following, we provide several points where the analysis could be further elaborated to establish clearer physical causality.

We thank Reviewer#1 for their constructive comments. We have carefully revised the manuscript (MS) and incorporated substantial additional analyses addressing the key points raised by the Reviewer. These include a more explicit treatment of the physical mechanisms controlling the nocturnal boundary layer, an extended climatological context, and a clearer quantification of the main drivers of ANBL variability. We believe that these additions significantly improve the robustness of the results and the physical interpretation, and that the actual revised manuscript addresses the concerns raised by the Reviewer. Below, we respond to each comment in detail and describe the corresponding changes implemented in the revised version of the MS. The line numbers referenced here are based on the revised version.

Specific comments

1. The study could benefit from an extended climatology of the stability of the ANBL. Based on only one La Nina year (2022) and one El Nino year (2023) it is hard to explain which part of the variability can be attributed to the ENSO and which part to the annual variability. With an elaborate description of the yearly variation, the ENSO effect could be clearly quantified.

We thank the Reviewer for their important comment. We agree that an extended climatology of ANBL stability is necessary to place the 2022 and 2023 results in the context of the background interannual variability. At the same time, we would like to clarify an observational limitation of the dataset. The full vertical profile of sonic anemometers up to 325 m at Amazon Tall Tower Observatory (ATTO) became operational only in August 2021. Therefore, reliable estimates of the nocturnal boundary-layer height (hn) are only available from 2022 onward. Although 2024 could provide an additional year of hn estimates, this year was also affected by the aftermath of the 2023 El Niño and cannot be treated as an independent climatological reference (Souza et al., 2024).

To address this limitation, we added an extended climatological analysis based on variables available over a longer period and directly linked to ANBL variability: nocturnal net radiation (Rn) and the atmospheric stability parameter (z/L). These variables provide important information about nocturnal radiative cooling and the atmospheric stability, both of which strongly influence ANBL behavior. This climatology was calculated for the 2016–2024 period using the same nighttime interval adopted throughout the manuscript (00:00–09:00 UTC). Figure 1 (of this document) shows that the dry season is generally characterized by higher negative net radiation values, consistent with stronger nocturnal radiative cooling, and by larger z/L values, indicating more stable conditions. The year 2023 shows z/L values above the climatological mean during most months, particularly from May onward, whereas 2022 remains generally closer to, or below, the climatological mean during several months. This additional analysis supports the interpretation that the shallower ANBL observed in 2023 was associated with enhanced nocturnal stability.

We included this discussion in the revised manuscript to place the analyzed years within the observed ATTO climatology context. Since radiative cooling and stability are relevant controls on nocturnal turbulence and ANBL structure, these deviations from the climatology can be associated to the observed differences in hn between 2022 and 2023.

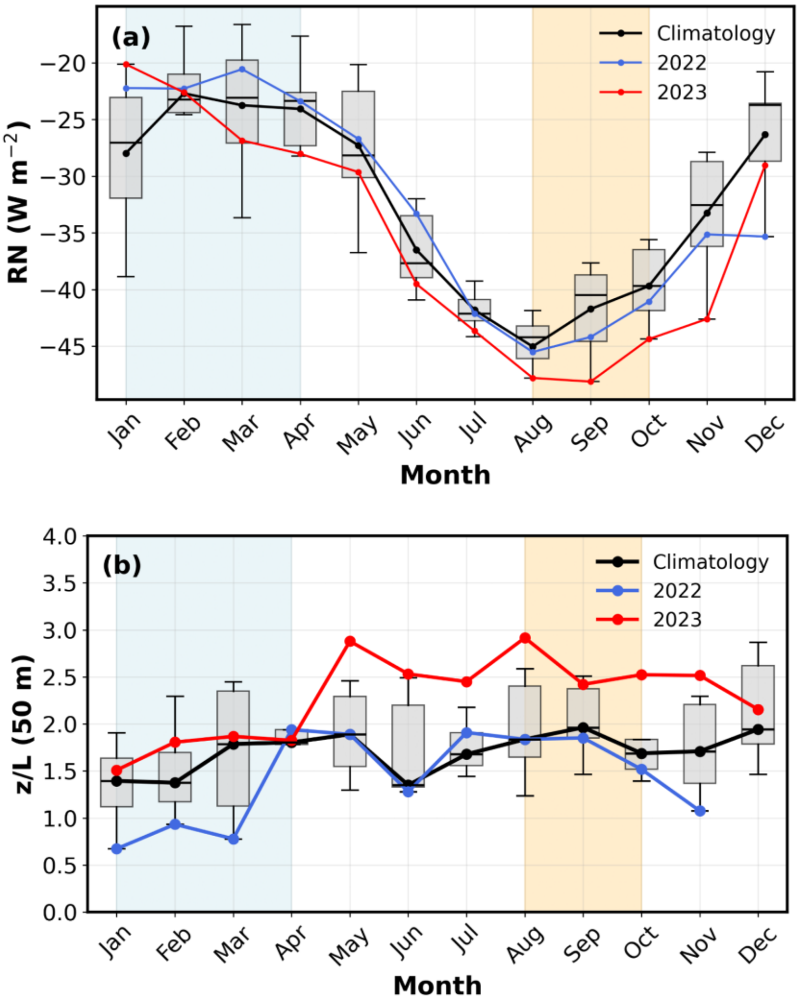

Figure 1 (Figure 3 in new version of the manuscript). Monthly mean of (a) net radiation (Rn) at 81 m and (b) stability parameter (z/L) at 50 m for the nighttime period (00:00–09:00 UTC). Grey boxplots represent the monthly climatological distribution for 2016—2024. Shaded blue and orange areas indicate the wet and dry seasons, respectively .

In the new version of the manuscript, it was added:

<u>L 187- 195</u>: To place the analyzed years in a broader climatological context, Figure 3 shows the monthly nocturnal climatology of Rn and z/L for the 2016–2024 period, using the same nighttime interval adopted in this study (00:00–09:00 UTC). The climatology highlights a clear seasonal cycle, with stronger nocturnal radiative cooling during the dry season associated with higher z/L values and therefore more stable atmospheric conditions. In 2023, z/L values were higher than the climatological mean during most months, especially from May onward, whereas 2022 remained closer to, or below, the climatological mean values. These departures from the ATTO climatology indicate that the two analyzed years experienced distinct nocturnal radiative cooling and stability conditions. Since Rn and z/L are relevant controls on turbulence

intensity and the vertical structure of the nocturnal boundary layer, these differences may be related to the contrasting hn behavior observed in 2022 and 2023 (discussed in section 3.2).

2. In relation to this a clearer identification and quantification of the main drivers would substantially strengthen the manuscript. For example, Figure 2 of this document presents longwave radiative cooling, but its role in enhancing nocturnal stratification is not sufficiently discussed. Further elaboration on how radiative cooling contributes to the stability of the nocturnal boundary layer would be valuable. Similarly, in lines 200–205, the manuscript discusses shear associated with changes in wind direction, which is a well-known mechanism for turbulence generation. Quantifying the magnitude of this shear using the available observations, and assessing its relative importance in sustaining turbulence and shaping the nocturnal boundary layer structure, would greatly improve the physical interpretation. We think here it can be convenient to connect and relate their findings with recent work of Mahrt and Acevedo (Boundary-layer Meteorology 187:141–161, 2023 and references therein).

We thank Reviewer #1 for this comment. To better quantify the main drivers of NBL evolution, we expanded the analysis of the two case-study nights showed in the previous version of the manuscript, including net radiation (Rn) at 81 m, cloud fraction (%), vertical profile of the potential temperature (θ), and vertical wind shear (dU/dz) for 18 and 25 August 2022 (Figure 2 of this document). To compute wind shear, third-order polynomial fits were applied to the wind speed profiles (U(z)), from which analytical vertical derivatives were calculated. Cloud cover was estimated from observations obtained by the Cloud Radar Profiler (METEK MIRA-35C) installed at the ATTO site. GOES-16 IR Channel 13 (10.3 µm) brightness temperature imagery was additionally used to illustrate cloud cover conditions during the two nights (Figures 3 and 4 of this document).

The night of 18 August 2022 represents a strongly stratified and more decoupled case compared to 25 August 2022. Strong radiative cooling (Fig. 2a), reduced cloud occurrence (Fig. 2c and Fig. 3), and a pronounced vertical potential temperature gradient (Fig. 2e), were associated with a shallow hn, mostly around 80–100 m. Despite the presence of wind shear at some levels, the strong thermal stratification suggests that mechanically generated turbulence aloft was not efficiently coupled downward to the layer near the canopy. This behavior is consistent with a layered nocturnal structure in which the shallow surface-based layer remains isolated from the air above, similar to the regime described by Mahrt and Acevedo (2023). In contrast, the night of 25 August 2022 showed larger cloud cover (Fig. 2d and Fig. 4), reduced radiative cooling during the early night (Fig. 2b), and weaker thermal stratification (Fig. 2f). Wind shear extended to higher levels (Fig. 2h), reaching approximately 150–170 m, close to h_N. This suggests that mechanical forcing contributed to sustaining turbulence over a deeper layer under weaker stratification. Therefore, the differences between those two nights are interpreted as the result of the balance between radiative cooling, which enhances thermal stratification and suppresses turbulence, and shear-generated mechanical turbulence, which can deepen or sustain the NBL when coupling is possible.

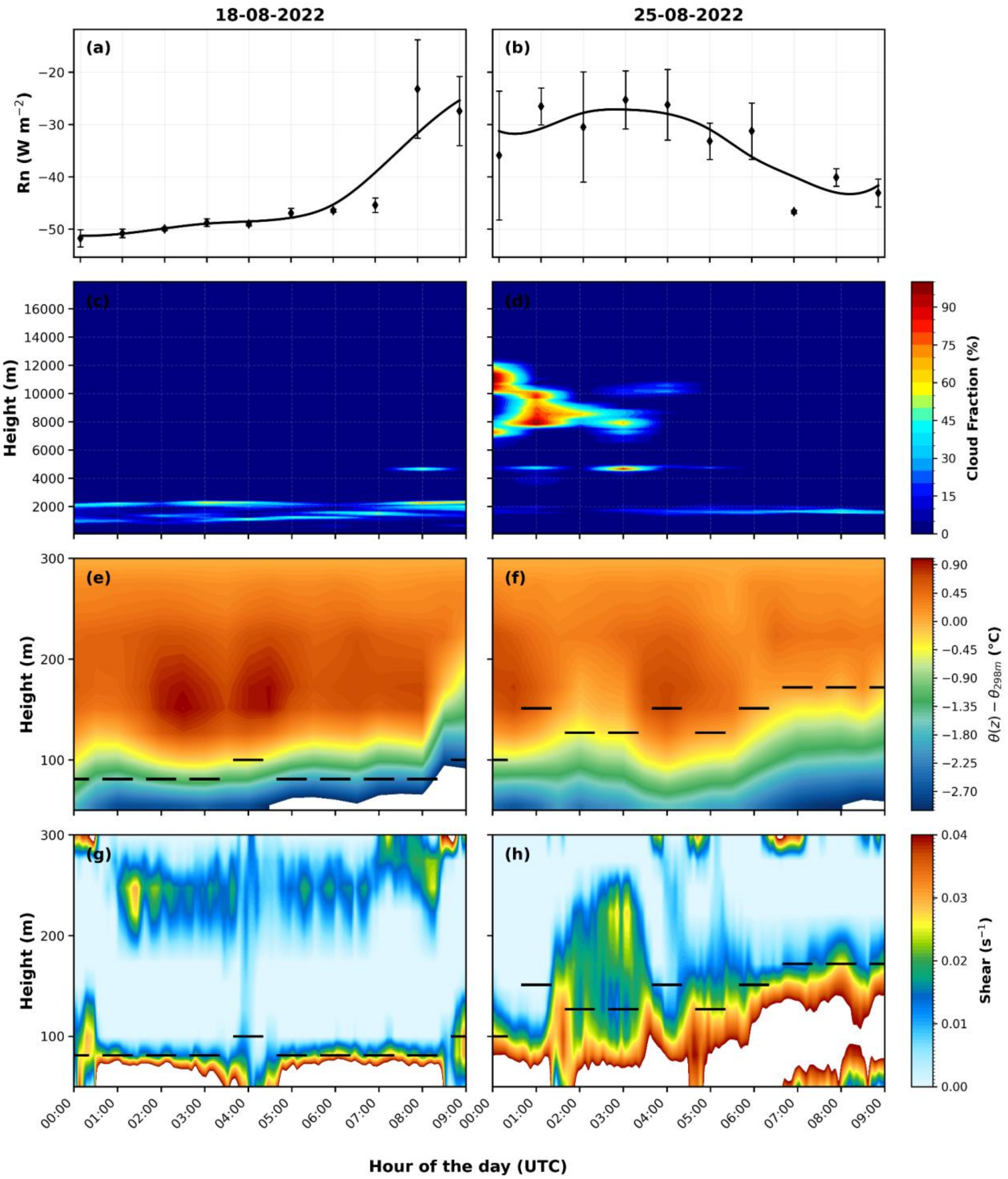

Figure 2 (Figure 9 in new version of the manuscript). Nocturnal evolution of (a, b) hourly mean net radiation (Rn) at 81 m (± standard deviation), (c, d) cloud fraction (%), (e, f) vertical potential temperature (θ) difference from the value observed at 298 m, and (g, h) vertical wind shear (dU/dz) during the case-study nights of 18 August 2022 (left panels) and 25 August 2022 (right panels). Black horizontal segments indicate the estimated nocturnal boundary layer height at each hour.

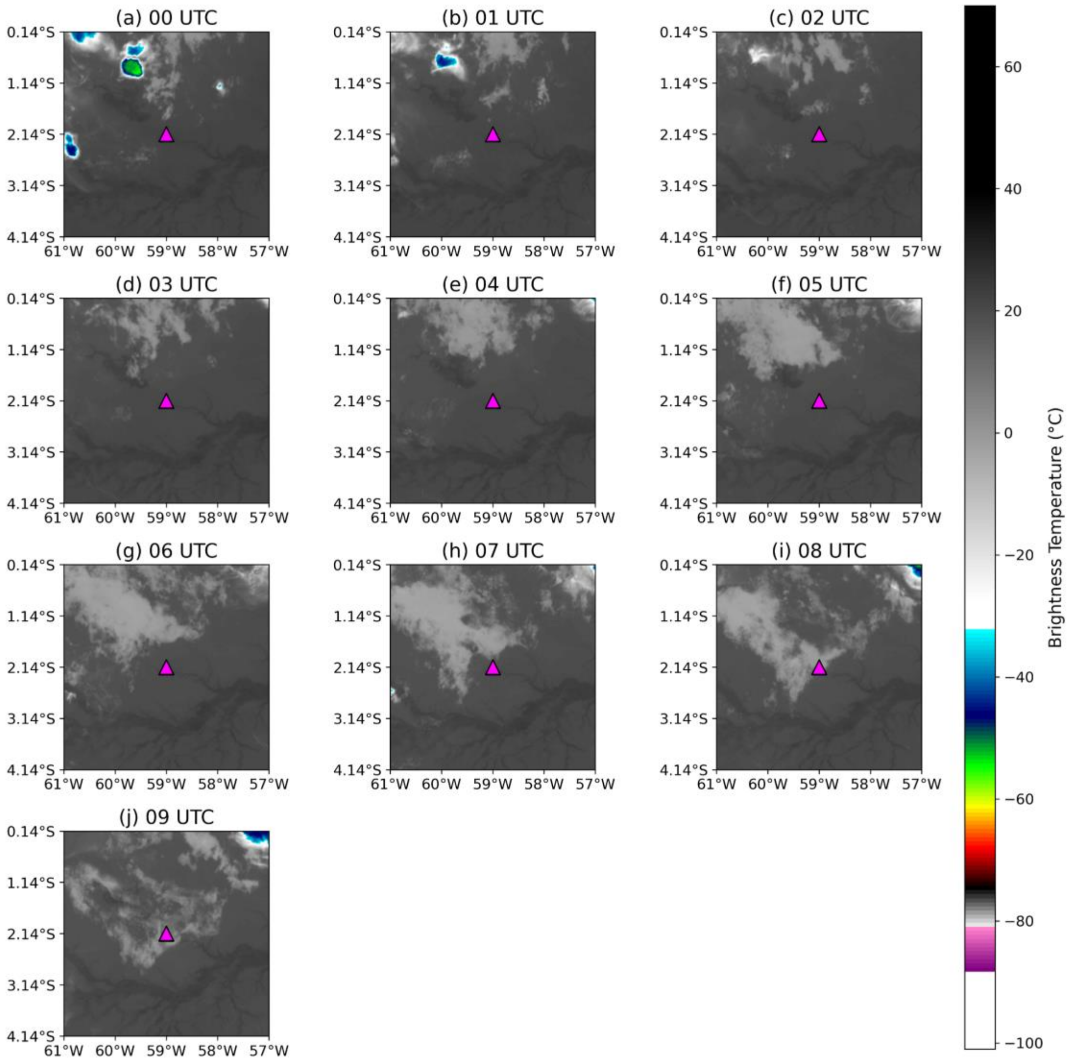

Figure 3 (Figure S2 in new version of the manuscript). GOES-16 IR Channel 13 (10.3 µm) brightness temperature over the ATTO site on 18 August 2022. Panels (a–j) show hourly images from 00 to 09 UTC. The magenta triangle marks the location of the ATTO tower.

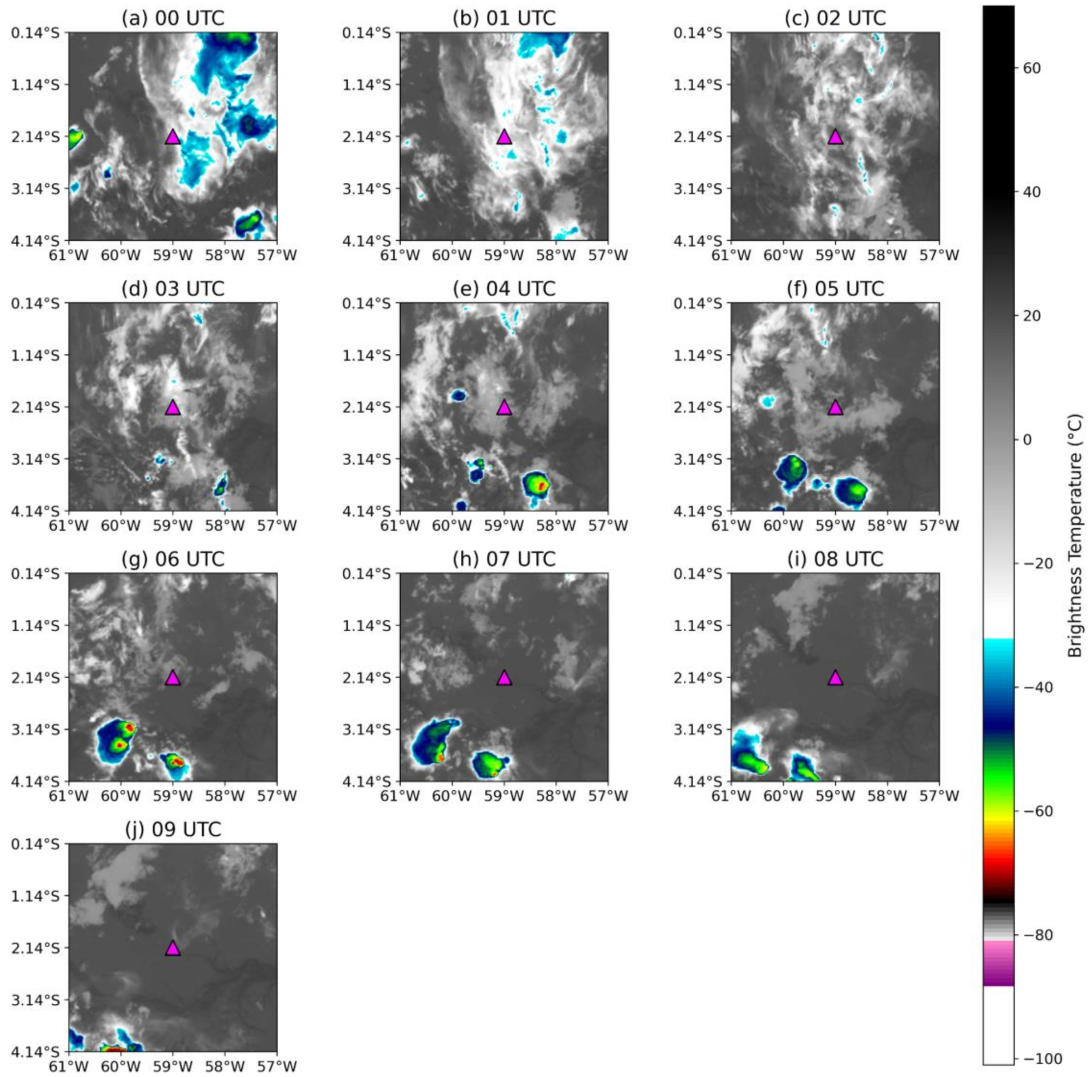

Figure 4 (Figure S3 in new version of the manuscript). GOES-16 IR Channel 13 (10.3 µm) brightness temperature over the ATTO site on 25 August 2022. Panels (a–j) show hourly images from 00 to 09 UTC. The magenta triangle marks the location of the ATTO tower.

We included this new analysis in Section 3.3 of the Results and in the new Discussion section of the revised manuscript.

L239–253: To better identify the main drivers controlling the contrasting hn behavior during the two case-study nights, we further ana lyzed Rn at81m,cloudcover,the vertical profile of θ and windshear (dU/dz) (Fig. 9). These variables provide complementary information on the local radiative forcing, cloud modulation of nocturnal cooling, thermal stratification, and mechanical turbulence generation. The night of 18 August 2022 was characterized by strong nocturnal radiative cooling (Fig. 9a), reduced cloud occurrence (Fig. 9c and Fig. S2), and a pronounced vertical potential temperature gradient (Figure 9e). These conditions indicate enhanced thermal stratification near the surface. Although wind shear was observed at some levels (Fig. 9g), the strong stratification suggests that mechanically generated turbulence aloft was not efficiently coupled downward toward the canopy. This supports the interpretation that the shallow hn observed on 18 August 2022 reflects not only strong thermal stratification, but also canopy-induced suppression of vertical mixing near the forest top. This configuration is consistent with a shallow surface-based nocturnal layer that remained partly decoupled from the air above, similar to the layered nocturnal structure described by Mahrt and Acevedo (2023). In contrast, the night of 25 August 2022 showed larger cloud cover (Fig. 9d and Fig.S3), weaker radiative cooling during the early part of the night (Fig. 9b), and weaker thermal stratification (Fig. 9f). Wind shear extended to higher levels (Fig. 9h), reaching approximately 150–170 m, close to the observed hn. This suggests that, under weaker stratification, mechanically generated turbulence was more effectively coupled over a deeper layer, contributing to the larger and more variable hn observed during this night.

L289-322: The results presented here demonstrate that the nocturnal boundary-layer height (hn) above the central Amazon is strongly controlled by the interaction between nocturnal radiative cooling, atmospheric stability, cloud cover, and mechanically generated turbulence. Although previous Amazonian studies have primarily focused on the daytime evolution of the atmospheric boundary layer (Fisch et al., 2004; Carneiro and Fisch, 2020; Dias-Júnior et al., 2022), our results show that the nocturnal boundary layer also exhibits pronounced seasonal and interannual variability, with important implications for turbulence exchange and trace-gas transport above tropical forests.

One of the clearest patterns observed in this study is the systematic reduction of hn during the Dry season and during the El Niño year (2023). These periods were characterized by stronger nocturnal net radiative loss (Figure 2a) and enhanced atmospheric stability, reflected by larger z/L values (Figure 2b) and a stronger thermal gradient (Fig. S6b, d). Under these conditions, turbulent exchange becomes increasingly suppressed, limiting the upward transport of sensible heat and favoring the formation of shallower nocturnal layers (Figures 4d and 5b). In contrast, wetter conditions, particularly during the Wet season of 2022, were associated with weaker radiative cooling (Figure 2a), reduced stability (Figure 2b), Weak thermal gradient(Fig S6a, c), and deeper nocturnal layers (Figures 4a and 5a). These findings reinforce the strong coupling between cloud cover, nocturnal cooling, and turbulence generation over the Amazon rainforest.

The hourly evolution of hn also reveals the importance of the temporal evolution of thermal stratification during the night. In all analyzed periods, hn was generally larger at the beginning of the night and progressively decreased toward the early morning hours (Figure 5). This behavior is particularly evident during the Wet season of 2022, when the thermal gradient remained relatively weak during the first hours of the night (Figures 9e,f and S6a), allowing mechanically generated turbulence to sustain a deeper nocturnal boundary layer. As the night progressed, radiative cooling intensified the thermal gradients, suppressing turbulence and leading to a gradual collapse of hn. This progressive reduction of turbulent mixing throughout the night is consistent with the classical evolution of stable nocturnal boundary layers described in previous studies (Mahrt, 1999; Sun et al., 2002).

The results also demonstrate that the interaction between thermal stratification and mechanically generated turbulence is fundamental for understanding the nocturnal boundary-layer structure above the Amazon forest (Figure 9). The case studies revealed that low-level jets (LLJs) (Figure 7) and enhanced vertical wind shear (Figure 9 g,h) may sustain turbulence above the canopy, but the influence of this turbulence on the lower nocturnal boundary layer depends on the degree of vertical coupling between atmospheric layers. This interpretation is consistent with the conceptual framework proposed by Mahrt and Acevedo (2023), in which nocturnal boundary layers may deviate from a vertically monotonic structure and instead exhibit layered configurations composed of shallow surface-based layers, transition layers, and elevated turbulent regions.

Our observations suggest that the forest canopy plays a key role in reinforcing this layered structure. Under strongly stable conditions, the canopy acts as a roughness and drag layer that attenuates momentum transfer toward the surface. Consequently, turbulence generated aloft by LLJs or strong wind shear may remain confined to elevated layers and may not efficiently penetrate downward through the canopy layer. This mechanism likely explains the shallow hn observed on 18 August 2022, when strong thermal stratification and weak vertical coupling produced a highly decoupled nocturnal structure. In contrast, on 25 August 2022, weaker thermal stratification allowed mechanically generated turbulence to penetrate deeper into the lower nocturnal boundary layer, resulting in larger and more vertically connected hn values.

3. In the results, Figure 4, which presents the nocturnal boundary layer height under wet and dry conditions for 2022 and 2023, would benefit from further elaboration. While the results are interesting, the discussion remains largely descriptive. A deeper analysis is needed to explain the origin of the observed differences. In particular, it would be valuable to discuss which physical processes may drive these contrasts and whether they can be linked to other controlling variables. In particular the role of locally driven processes such as stability, turbulence, surface fluxes, or large-scale meteorological conditions, that influence the ANBL.

Our analyses indicate that the seasonal and interannual variability of the ANBL is strongly linked to the modulation of nocturnal radiative forcing by cloud cover. Wetter conditions, associated with increased cloudiness, reduce net longwave radiative loss at the surface, weakening near-surface cooling and limiting the development of strong thermal stratification. In contrast, clearer conditions during the dry season favor stronger radiative loss and a more stable nocturnal boundary layer.

These large-scale meteorological conditions directly influence the efficiency of local turbulent processes controlling hn. Under weaker stability, turbulence generated by wind shear can more effectively maintain vertical mixing and sustain a deeper nocturnal layer. Conversely, under strongly stable atmospheric conditions, turbulence is suppressed, vertical exchange becomes less efficient, and the ANBL remains shallower.

The case studies analyzed in response to Reviewer Comment (2) support this interpretation by showing that deeper hn values are associated with weaker stability and enhanced turbulent mixing, whereas shallower hn occurs during nights characterized by stronger thermal stratification. Based on these results, we interpret the deeper nocturnal layers observed during the wet season of 2022 as a consequence of reduced radiative cooling and weaker stability, while the shallower hn observed during the dry season of 2023 reflects enhanced radiative cooling and stronger suppression of turbulence. We revised the manuscript to make these physical links clearer in the Results and Discussion sections

We have added a new discussion addressing this point in the revised version of the manuscript (lines 174–222 of this document).

4. In the same line, and perhaps to support their analysis, perhaps it is interesting to study if there are current formulations (representations) or other methods to estimate the NBL height that are able to reproduce the observational dynamic evolution.

We thank the reviewer for this suggestion. We now added a short discussion of this point in the manuscript.

Several methods can be used to estimate hn, including criteria based on potential temperature, CO2, wind speed, Richardson number, and TKE. A recent study at ATTO using field data collected during CloudRoots-Amazon22 (Vila-Guerau de Arellano et al., 2024) observations applied these five criteria and showed that they reproduce the hourly evolution of the nocturnal boundary-layer height, with values ranging from 114 to 241 m and mean estimates between 150 and 188 m (Figure 2 of the Huitema et al., 2026). The same study also showed that hn was shallower under strongly stable conditions and deeper under weakly stable conditions, consistent with the expected stability-turbulence control.

In our study, we decided to use the sensible-heat-flux profile method because it is directly linked to the turbulent definition of the nocturnal boundary layer. This choice is also supported by Mendonça et al. (2025, 2026), who showed that vertical profiles of sensible heat flux can be used to estimate hn at ATTO. Therefore, although other diagnostic methods are available and can reproduce the dynamic evolution of the NBL, we retained the heat-flux-based method because it provides a direct turbulence-based estimate and is consistent with previous ATTO studies.

we added this paragraph in the manuscript:

L344-354: Compared to previous Amazonian studies, the turbulence-based methodology adopted in this work provides an important advantage because it estimates hn directly from the vertical decay of turbulent sensible heat fluxes. Most previous studies relied on indirect methods based on thermodynamic profiles, Richardson number, or remote sensing approaches (Santos et al., 2007; Dias-Júnior et al., 2022). More recently, Mendonça et al. (2025) used the same turbulence-based methodology and reported hn values ranging between approximately 81 and 223 m, demonstrating the importance of surface roughness and topography for nocturnal boundary-layer structure. However, their study did not focus on the hourly evolution of hn or on its relationship with trace-gas concentration profiles. In addition, Huitema et al. (2026), using CloudRoots-Amazon22 observations (Vila-Guerau de Arellano et al., 2024), showed that multiple criteria based on potential temperature, CO2, wind speed, Richardson number, and turbulent kinetic energy reproduce similar nocturnal boundary-layer dynamics, with estimated values between 114 and 241 m. The agreement between these independent approaches and the results presented here supports the robustness of the observed dynamic evolution of hn at the ATTO site.

5. In section 3.3 the role of the canopy deserves more explicit attention. Given the observational setup, the authors are in a unique position to assess how the forest canopy influences the structure and dynamics of the nocturnal boundary layer (see for instance line 179 and 225). Although the results (line 223-228) conclude that the canopy plays a role, this influence is not sufficiently specified or supported by analysis. A more detailed discussion, ideally supported by quantitative evidence, of the mechanisms through which the canopy affects nocturnal stratification, turbulence, or mixing would substantially strengthen the manuscript.

In the revised manuscript, we expanded Section 3.3 to better describe the physical mechanisms through which the Amazon forest canopy influences nocturnal stratification and turbulent mixing. The tall and dense canopy strongly modifies the exchange of momentum and heat enhancing the vertical coupling/decoupling between the surface layer and the atmosphere aloft under stable nighttime conditions.

Our analysis indicates that during nights with stronger radiative cooling and enhanced thermal stability, turbulence generated above the canopy was not efficiently transported downward through the canopy layer. Under these conditions, the canopy acts as a barrier to vertical mixing, favoring the formation of a shallow and strongly stratified nocturnal layer close to the forest top. This behavior was particularly evident on 18 August 2022, when strong thermal stratification and weak cloud cover were associated with shallow hn values around 80–100 m. In contrast, during nights with weaker stability and enhanced wind shear, mechanically generated turbulence was able to remain coupled across a deeper layer above the canopy. Under these conditions, the canopy-induced decoupling was weaker, allowing turbulence to extend to higher levels and contributing to deeper and more variable hn values, as observed on 25 August 2022.

To support this interpretation, we added new analyses of vertical profile of the potential temperature gradients, wind shear, cloud fraction, and radiative forcing (Figure 2). These additional results provide quantitative evidence that the canopy influence on hn emerges from its interaction with thermal stratification and mechanical turbulence generation, rather than from a purely local surface effect.

We already added this discussion in part of the answers of the Comment (2)

L316-323: “Our observations suggest that the forest canopy plays a key role in reinforcing this layered structure. Under strongly stable conditions, the canopy acts as a roughness and drag layer that attenuates momentum transfer toward the surface. Consequently, turbulence generated aloft by LLJs or strong wind shear may remain confined to elevated layers and may not efficiently penetrate downward through the canopy layer."

6. Finally, additional background information would strengthen the results in Figure 8, which compared to two stability cases. More emphasis should be placed on the different background concentrations during the past days of the gases and their effect on the current nocturnal gas exchange. In addition, to truly understand the effect of stability on trace gas concentrations, it would be valuable to compare two nights with similar wind and background trace gas conditions. Especially, because previous papers highlight the complicated CH4 signal at ATTO with winds from the South-East (Botia et al., 2020).

We agree with the reviewer that it would be valuable to compare nights with similar wind and background trace gas conditions. However, due to the large natural variation of CO and CH_4 concentrations, this is challenging. In the previous version of the manuscript, we included a multi-day figure showing the CO and CH_4 concentrations before and during each case study (Discussion paper, Figure S4) which indeed shows that the starting background conditions were not the same for the two case studies.

The initial conditions of the first case study (Aug 18, 2022) were with non-elevated concentrations at all levels. Then, an air mass with slightly enriched CO and CH_4 reached the ATTO fieldsite. This night had a shallow hn (80-100 m), together with stronger thermal stratification, which limited the vertical exchange between the lower and upper layers. As a result, elevated CO and CH_4 concentrations were only observed at the upper sampling levels, while the lower levels remained unaffected.

For the Aug 18, 2022 case, the multi-day background concentrations were already elevated before the selected night, and the lower measurement levels had likely been influenced by trace-gas-enriched air during the previous days. Therefore, the higher CO and CH_4 concentrations observed near the canopy at the beginning of the night are interpreted as a residual effect of previous plume influence combined with slower ventilation of the lower canopy layer. This interpretation is consistent with the slower wind speed near the canopy compared to higher levels, as discussed in the manuscript.

While the gas concentration profiles support and help visualize the estimated boundary layer height, we recognize that the observed concentration patterns are more complex and, as the reviewer noted, are also influenced by factors such as background concentrations, wind directions, source regions and residual effects from previous nights. For this reason, we refer to the gas concentration profiles as supporting evidence for the validity of the estimated boundary layer height, rather than as a direct or exclusive indicator.

Additionally and following the reviewer's comment, we did the following analysis/discussions to improve section 4 of the manuscript (L330-345 of the new version of the manuscript). First, we now better acknowledge the complexity of CH_4 and CO signals at ATTO as also highlighted by Botía et al. (2020). Second, in the revised manuscript, we highlight that our main focus is on the interpretation of the vertical gas concentration gradients (differences between upper and lower layers), rather than absolute concentration values. Lastly, we added two additional case studies to the supplement, namely the nights of Aug 28 and Sept 2, 2022.

The case studies were selected to provide an additional comparison of nights with different thermal stability and hn behavior. Changes in hn are controlled by a combination of drivers, including cloud cover, wind shear, radiative cooling, and thermal stratification. These factors can either enhance or reduce the nocturnal boundary layer height. This point was already discussed in our response to Comment (2). Following this interpretation, for the two selected cases we now include representative temperature-gradient profiles to illustrate the thermal stability conditions associated with each case. On 02 September 2022, the nocturnal boundary layer remained shallow, mostly around 80-100 m, and the potential temperature gradient was stronger, reaching values close to -4 K near the canopy (Figure 6a in this document). In this case study, the upper levels (273 and 321m) consistently showed an independent behaviour in comparison to the lower levels (Figure 5a and 5c in this document), indicating that the shallow and stable layer acted as a barrier to vertical exchange (Figure 7a and 7c in this document).

In contrast, on Aug 28, the potential temperature gradient was weaker, approximately −2 K (Figure 6b in this document) near the canopy top, hn was deeper and more variable, and decreasing during the night. This temporal behaviour is visible also in the gas concentrations, especially for CH_4, showing a large enhancement at 273 m and 321 m of maximum 200 ppb. At the same time ~5:00 UTC the hn separated the upper levels from the lower levels, after which the former decoupled, likely due to the arrival of an enriched air mass.

These two additional cases also exemplify the interaction between the hn and the initial or background concentrations prior to the evolution of the nocturnal event. In the first one (02.09.2022) the initial concentrations are relatively high, since previous hours, at all levels (~290 ppb CO and ~2050 for CH_4) compared to the rest of the night. The weak decoupling (~40 ppb in both CH_4 and CO) between 273-321 m and the levels below, is due to the shallow hn (80-100 m) which disconnects the layers closer to the canopy, with low CH_4 and CO, and leading to a dilution of the initial mole fractions at the levels below 273 m. In contrast, the trace gases at 273-321 m remain with small variability relative to their initial state because the measurement height is above the hn. Now, in the second event shown (28.08.2022), the initial concentrations are low at all levels (close to ~122 ppb CO and ~1950 ppb CH_4) and thus the change in hn at 05:00 UTC led to an abrupt enhancement (~200 ppb in CH_4) at 273 m and 321 m, which we interpret either as a signal from the previous day that remains in the residual layer or, and even more likely, a change in wind direction that brings signals from a methane source. Here the new text addition that we have included in the revised manuscript:

L328-343: The interpretation of these concentration patterns must also consider the background atmospheric composition during previous days. As discussed by Botía et al. (2020), the ATTO site frequently experiences nighttime CH4 accumulation associated with strong thermal stratification, suppressed turbulence, and horizontal transport from likely wetland source regions. In addition, CO concentrations are strongly influenced by regional biomass-burning plumes (Andreae et al., 2015; Van Asperen et al., 2024). For example, the elevated CO and CH4 concentrations observed on 25 August 2022 likely reflected the residual influence of previous plume events (Figure S5)) combined with slower ventilation near the canopy. Therefore, rather than associating multi-day concentration variability directly with hn, our interpretation focuses on the short-term vertical concentration gradients and their relationship with nocturnal turbulent structure. The additional case studies presented in the Supplement further reinforce this interpretation (Fig. S7). Strongly stable nights with shallow hn (Fig. S8a) exhibited clear vertical separation between upper and lower layers (Fig. S7a,c), while less stable nights with deeper hn (Fig S8b) showed much more homogeneous concentration patterns throughout the tower profile (Fig. S7b, d). The supplementary cases also show the importance of the initial/background concentrations from the previous days in shaping the nocturnal CO and CH4 profiles (Fig. S9). As in the 18 and 25 August cases, the vertical gradients were influenced not only by the evolution of hn, but also by the concentration structure already present before the night. These consistent relationships between hn and the observed concentration gradients provide independent observational support for the turbulence-based estimates of nocturnal boundary-layer height presented here.

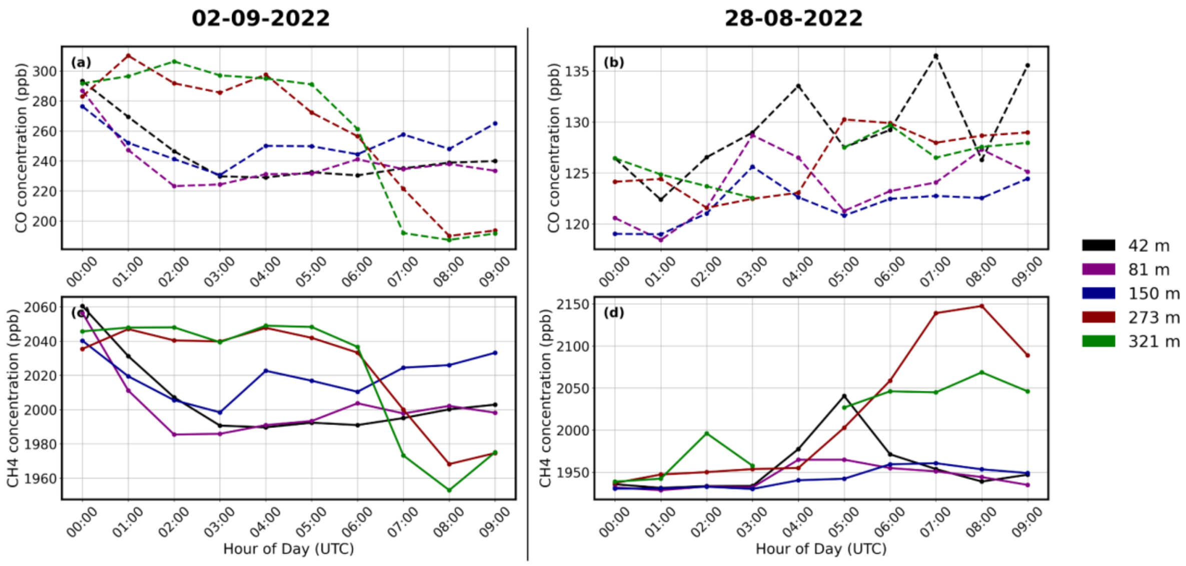

Figure 5 (Figure S7 in the new version of the manuscript).Hourly mean vertical profiles of CO and CH4 concentrations during two additional nocturnal case studies: 02 September 2022 and 28 August 2022. Panels (a) and (b) show CO and CH4, respectively, for 02 September 2022, while panels (c) and (d) show COand CH4, respectively, for 28 August 2022

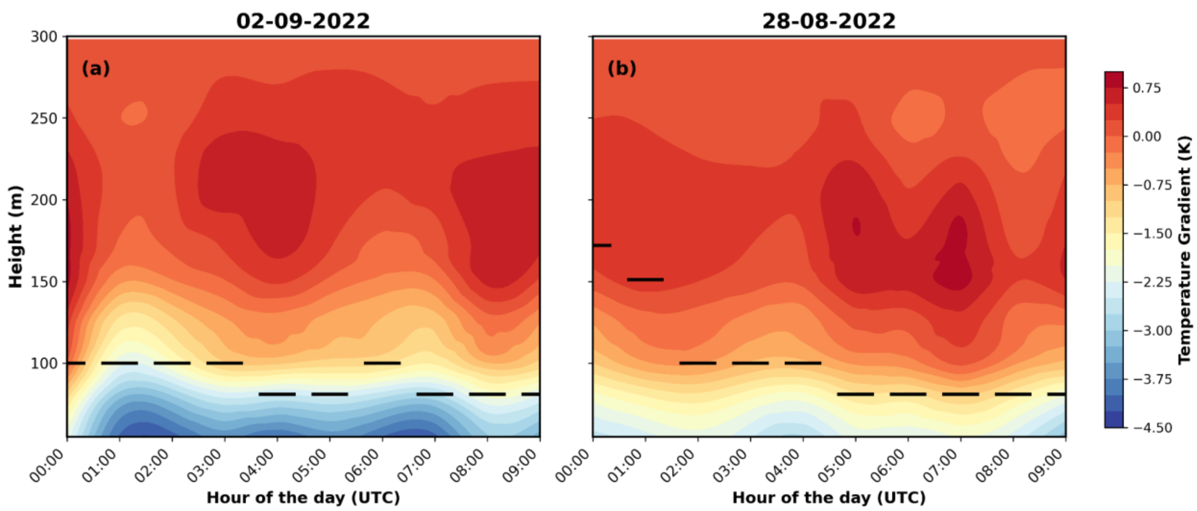

Figure 6 (Figure S8 in the new version of the manuscript. Time-height evolution of the vertical potential temperature gradient during the nights of 02 September 2022 and 28 August 2022. Panels (a) and (b) show the respective nights, with dashed black lines indicating the estimated nocturnal boundary-layer height hn

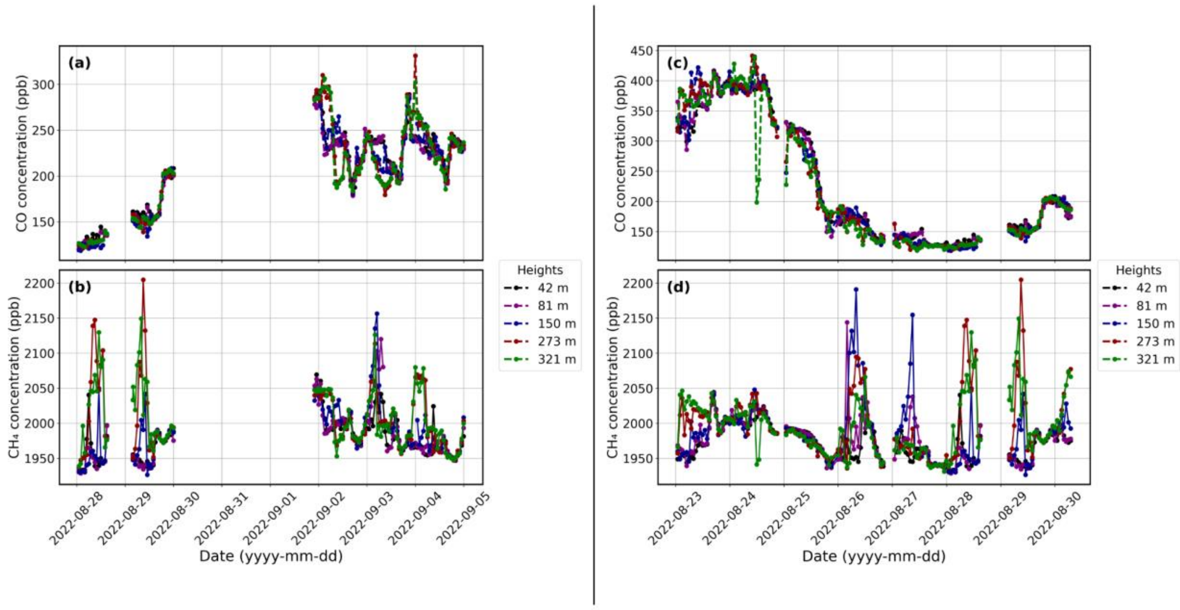

Figure 7 (Figure S9 in the new version of the manuscript). Multi-day evolution of CO and CH4 concentrations at different sampling heights before and during the selected nocturnal case studies. Panels (a) and (b) show CO and CH4, respectively, for the period including 02 September 2022, while panels (c) and (d) show COandCH4,respectively, for the period including 28 August 2022.

References:

Botía, S., Gerbig, C., Marshall, J., Lavric, J. V., Walter, D., Pöhlker, C., ... & Acevedo, O. C. (2020). Understanding nighttime methane signals at the Amazon Tall Tower Observatory (ATTO). *Atmospheric Chemistry and Physics*, *20*(11), 6583-6606.

Mendonça, A., Dias, C. Q., Acevedo, O. C., Marra, D. M., Cely-Toro, I. M., Fisch, G., ... & Mortarini, L. (2025, January). Nocturnal Boundary Layer Height Estimated from Direct Turbulence Measurements at the ATTO Tower. In *105th Annual AMS Meeting 2025* (Vol. 105, p. 446515).

Mendonça, A. C., Dias-Junior, C. Q., de Oliveira, M. I., Maroneze, R., Martins, L. G. N., Marra, D. M., ... & Acevedo, O. C. (2026). Is Low-Level Jet height a good approximation for the top of the nocturnal boundary-layer?. *Agricultural and Forest Meteorology*, *380*, 111065.

Huitema, A. C., de Feiter, V. S., González-Armas, R., Hartogensis, O. K., van Asperen, H., Quaresma Dias-Júnior, C., & Vilà-Guerau de Arellano, J. (2026). CO 2 and Heat exchange across the Nocturnal Canopy–Atmosphere interface in the Amazon rainforest. *EGUsphere*, *2026*, 1-32.

Mahrt, L., & Acevedo, O. (2023). Types of vertical structure of the nocturnal boundary layer. *Boundary-Layer Meteorology*, *187*(1), 141-161.

Souza Jr, C. M., Marengo, J., Ferreira, B., Ribeiro, J., Schirmbeck, L. W., Schirmbeck, J., ... & Latuf, M. O. (2024). Amazon severe drought in 2023 triggered surface water loss. *Environmental Research: Climate*, *3*(4), 041002.

Vila-Guerau de Arellano, J., Hartogensis, O. K., De Boer, H., Moonen, R., González-Armas, R., Janssens, M., ... & Röckmann, T. (2024). CloudRoots-Amazon22: Integrating clouds with photosynthesis by crossing scales. *Bulletin of the American Meteorological Society*, *105*(7), E1275-E1302.

Review of MS. MS No.: EGUSPHERE-2025-6531

Title: Estimation of Nocturnal Boundary Layer Height in the Central Amazon, Supported by Gas Concentration Profiles

Response (blue color) to anonymous **Referee #2** (black). The original manuscript was changed accordingly.

General comments

This manuscript by Carla Souza et al. investigates the height of the nocturnal boundary layer (hn) above the central Amazon using micrometeorological observations from the Amazon Tall Tower Observatory. By analyzing vertical profiles of turbulent sensible heat flux up to 300 m, the authors estimate hn more directly than many previous studies that rely on indirect proxies. The analysis focuses on seasonal differences between wet and dry periods during one La Ni˜na year and one El Ni˜no year. The authors report substantial variability in nocturnal boundary layer height, with the largest values occurring during the wet season of the La Niña year (approximately 270 ± 40 m) and the smallest during the dry season associated with El Ni˜no (approximately 100 ± 27 m). They further show that variations in hn influence the vertical distribution of CO and CH4, with the boundary layer height acting as a barrier that can limit the exchange of air masses containing elevated trace gas concentrations. Overall, the study provides observational evidence of strong seasonal and interannual variability in the nocturnal boundary layer over the Amazon and highlights implications for the representation of boundary layer processes and trace-gas transport in atmospheric models.

The manuscript addresses an interesting and relevant topic; however, substantial revisions are required before it can be considered for publication. In its current form, the study would benefit from more in-depth investigation of the underlying physics and in-canopy processes. The analysis appears somewhat limited, and important mechanisms are not sufficiently explored or supported. Additionally, the manuscript is relatively short for a full paper, and several limitations of the study are not adequately discussed. Expanding on these aspects would improve the rigor and clarity of the work. While I find some of the ideas promising and appreciate the effort, there are a number of significant points that must be clarified. I would like to see detailed responses to the comments provided below, as they are essential for properly evaluating the study.

Given the scope and depth of the current manuscript, I suggest that the work may be more suitable for consideration as a letter rather than a full research article. Below are my specific comments:

We thank Reviewer #2 for the careful evaluation of our manuscript and for the constructive comments. We appreciate the reviewer's positive assessment of the relevance of the topic and of our observational approach to estimate the nocturnal boundary-layer height from vertical profiles of turbulent sensible heat flux.

Following the reviewer's suggestions, we have revised the manuscript to strengthen the physical interpretation of the results and to better discuss the mechanisms controlling hn. In particular, we expanded the discussion of thermal stability, turbulence, wind shear, radiative cooling, seasonal/interannual variability, and their implications for trace-gas transport. We also added supporting analyses and clarified the limitations of the study. Regarding the suggestion that the manuscript may be more suitable as a letter, we respectfully believe that the revised version is now appropriate as a full research article.

All comments have been addressed below, and the manuscript has been revised accordingly.

Specific comments

• Lines 24-25: Attribute the reported differences of zi between pastures and forests patches to the physical implications. It is also useful to define how zi is calculated in the literature

We agree with the reviewer and updated the text in the revised manuscript as detailed below:

L26-30: " estimated zi from radiosonde data as the height of the main inversion layer, identified from the vertical profile of potential temperature. They showed that zi values differ between pasture and forest areas, with a deeper boundary layer over pasture, up to ~1650 m, compared to forest, ~1100 m. This contrast is attributed to differences in surface energy partitioning, since pasture areas exhibit higher sensible heat fluxes and lower evapotranspiration compared to forests, leading to stronger thermal turbulence and enhanced boundary layer growth. ."

• Line 35: zi and not Zi

Thank you for pointing this out. This has been corrected in the revised manuscript (L39).

• Line 61: Again, mention how Mendonça et al. defined the calculation of zi

We clarified this point in the revised manuscript by rephrasing the sentence as follows:

L60-61: "These estimates are based on the height at which H falls below 5% of its near-surface value "

• Line 82: Define the air temperature variable symbol (T).

Thank you for pointing this out. This has been corrected in the revised manuscript (L89).

• Line 94: Is 30-min your Reynolds average? Any double rotation of the wind is attempted? Linear detrending ?

We thank the reviewer for this question. The 30-minute subsets (18000 records) were not used as Reynolds averaging intervals, but for quality control (QC) procedures following Vickers and Mahrt (1997) and Zahn et al. (2016), including checks of data completeness, identification of error flags, spike detection and removal, and stationarity tests. After QC, the planar fit method (Wilczak et al., 2001) was used for tilt correction. For each six-month period, wind velocity components were used to estimate the anemometer tilt angles and define a mean streamline coordinate system. The tilt-corrected wind vectors were then rotated for each 30-min interval to align the horizontal wind component with the mean wind direction (Kaimal & Finnigan, 1994). Subsequently, linear detrending was applied to 5-minute time windows, within which turbulent fluctuations and statistics were calculated.

The following sentence has been updated to the revised manuscript:

L105-118: “As in other micrometeorological studies (Foken and Mauder, 2008; Starkenburg et al., 2016; Dias et al., 2023), the high frequency data were initially segmented into 30-minute intervals (totaling 18000 measurements) for the application of quality control (QC) procedures and tilt correction. QC was performed for each wind component and for the temperature measured by the sonic anemometers. The QC process included verification of record integrity, detection of error indicators, identification and removal of spikes, as well as the application of stationarity tests. For a detailed description of the quality control protocol adopted at the ATTO Site, it is recommended to consult Zahn et al. (2016) and Dias et al. (2023).
After QC, the planar fit method (Wilczak et al., 2001) was used for tilt correction. For each six-month period, wind velocity components were used to estimate the anemometer tilt angles and define a mean streamline coordinate system. The tilt-corrected wind vectors were then rotated for each 30-min interval to align the horizontal wind components with the mean wind direction (Kaimal and Finnigan, 1994). Subsequently, turbulence statistics were calculated over 5-minute windows using Reynolds averaging, after applying linear detrending within each window. This shorter time window reduces the influence of non-turbulent motions, which are relevant under stable boundary layer conditions (Sun et al., 2002; Oliveira et al., 2018).”

• Line 100: 5-min turbulence statistics .. clarify how does it differ from the above 30-min Reynolds average? Delineate clearly between QC and Reynolds averaging. Justify these choices.

We thank the reviewer for these points. As clarified above, 30-minute blocks were used exclusively for QC procedures, whereas turbulence statistics were computed over 5-minute windows. This choice was made to better capture turbulent fluctuations while minimizing contamination from non-turbulent motions, which are relevant under stable boundary layer conditions (Sun et al., 2002; Oliveira et al., 2018). We have incorporated these clarifications into the revised manuscript, as detailed in our response to the previous comment (L584 this document).

• Line 116: Justify these thresholds and the sensitivity to these thresholds.

We thank the reviewer for the opportunity to clarify this point. The filtering thresholds were defined from the observed distribution of sensible heat flux (H) at each height range, while accounting for the expected decrease in flux magnitude with height above the canopy.

To test the sensitivity of hn to these thresholds, we applied two additional filtering scenarios. The baseline thresholds were −50 to 0 Wm^{-2} for 50–81 m, −30 to 10 Wm^{-2} for 100–151 m, and −20 to 10 Wm^{-2} for 172–298 m (Scenario 3). The permissive scenario expanded these ranges to −60 to 20, −45 to 25, and −35 to 15 Wm^{-2} (Scenario 2) respectively. The restrictive scenario reduced them to −30 to 0, −20 to 5, and −10 to 5 Wm^{-2} (Scenario 1), respectively.

The sensitivity test shows that the normalized heat-flux profiles and the estimated hn are very similar across the three scenarios (Figure 1). The difference in estimated hn was less than 15 m. This indicates that the main results are robust and not sensitive to the specific filtering thresholds used.

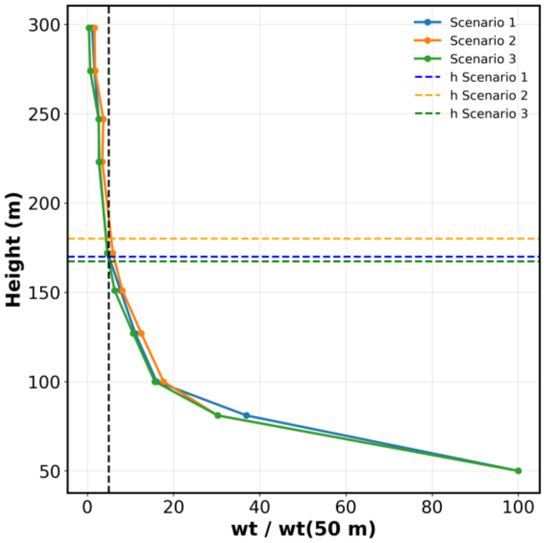

Figure 1. (Figure S1 in the new version of the manuscript) Sensitivity analysis of the filtering thresholds applied to the sensible heat flux (H). The normalized profiles (H/H50×100) are shown for three scenarios: the original thresholds (−50 to 0 W m−2 for 50–81 m, −30 to 10 W m−2 for 100–151 m, and −20 to 10 Wm−2 for172–298 m;Scenario 3), a more permissive scenario (−60 to 20, −45 to 25, and −35 to 15 W m−2; Scenario 2), and a morerestrictive scenario (−30 to 0, −20 to 5, and −10 to 5 Wm−2; Scenario 1). Dashed horizontal lines indicate the corresponding hn values.

We added this justification and the sensitivity analysis to the revised manuscript and included the figure in the Supplementary Material.

L 136-140: "To test the sensitivity of hn to these filtering limits, we applied a more permissive scenario (−60 to 20, −45 to 25, and −35 to 15 W m−2; Scenario 2) and a more restrictive scenario (−30 to 0, −20 to 5, and −10 to 5 W m−2; Scenario 1) for the three height ranges. The normalized profiles were very similar, and the estimated hn differed by less than 15 m among scenarios (Fig. S1), indicating that the results are robust to the selected thresholds. Th
"

• Line 142: There is another definition of hn as the height at which TKE drops below a certain percentage of the measured TKE near the surface. Why this criterion is not adopted ? Also, how would the results change based on the latter? In this context and since TKE friction velocity a measure of the shear strength, did you look at Richardson number that shows the competition between buoyancy and shear?

We appreciate the reviewer's suggestion. Indeed, both the sensible heat flux (H) and the turbulent kinetic energy (TKE) can be used to characterize turbulence. The H decreases with height and approaches zero at the level where turbulent mixing is suppressed, providing a direct indication of the NBL top (Fig. 2a). In contrast, although TKE also decreases with height, it does not become negligible at the NBL top (Fig. 2b), because non-turbulent motions can still contribute to velocity variances above this level (Acevedo et al., 2016).

This limitation has already been evaluated for the ATTO site. Huitema et al. (2026), analyzing observations during the dry season of 2022, estimated hn using different approaches and compared them against a reference hn derived from potential temperature profiles. Using a TKE-based criterion defined as the height where TKE is reduced to 20% of its canopy-top value, they found that this approach overestimates hn by approximately 18%. In addition, a Richardson number (Ri)-based criterion, defined as the lowest level where Ri ≥ 0.25, underestimates hn by approximately 19% (their Fig. 2). For this reason, we adopt H as the primary criterion, as it better represents the upper limit of turbulent mixing in the NBL.

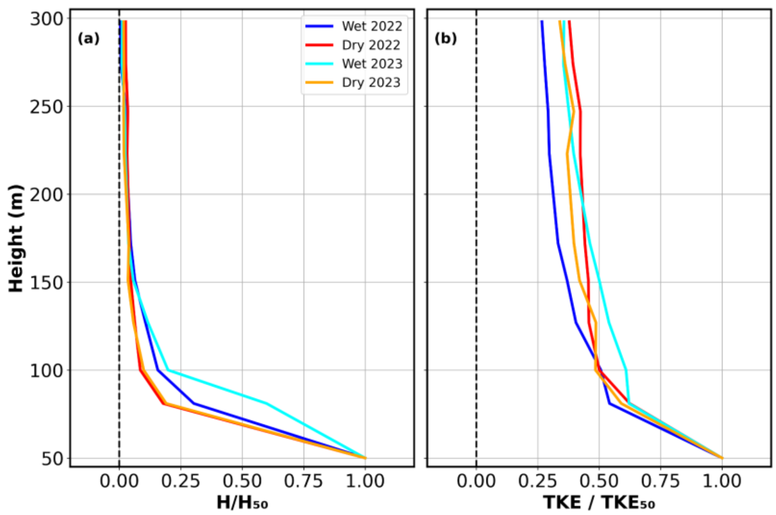

Figure 2. Average vertical profiles of normalized a) sensible heat flux (H) and b) turbulent kinetic energy (TKE) for wet and dry seasons in 2022 and 2023.

• Line 159: Report the value ζ = z/L

We thank the reviewer. In the revised manuscript, we have included quantitative values of the (z/L)

L184: "The Wet period is less stable (smaller z/L = 2.15), while the Dry period shows stronger stability (z/L = 3.10) "

• Line 163: After looking at figure 3, the results look so sensitive to the choice of 5% ! Without loss of generality, if you opted to choose 6% for example, the reported values would drastically change. Any thoughts?

We thank the reviewer for the opportunity to clarify the 5% threshold used to estimate hn.

The choice of the 5% threshold was based on previous studies (i.e. Nieuwstadt, 1984; Lenschow et al., 1988) since it reflects a point where turbulence, although still present, has significantly diminished relative to surface values (Stull 1988; Kaimal & Finnigan, 1994). Furthermore, this threshold offers a standardized method for defining hn, facilitating comparisons across different regions. Figure 3 of this document shows a normalized vertical profile of the sensible heat flux ($\overline{w'T'}$) using the flux value at 50 m as the reference (100%). The percentages on the x-axis represent the relative contribution of $\overline{w'T'}$ at each height compared to 50 m. The results demonstrate that hn estimates using the 3%, 5%, and 7% thresholds vary by less than 30 meters highlighting the robustness of the method.

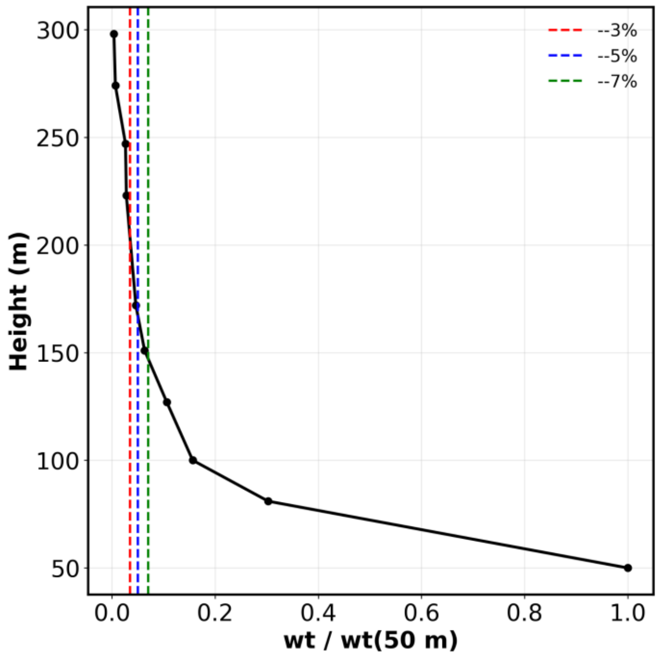

Figure 3. Normalized vertical profile of the sensible heat flux ($\overline{w'T'}$). The dashed vertical lines indicate thresholds at 3% (red), 5% (blue), and 7% (green) of the flux.

• Line 175: Compute the shear and relate to ζ = z/L

We thank Reviewer #2 for this comment. The atmospheric stability parameter (ζ = z/L) was already included in the Supplementary Material (Figure S1 of the previous version of the manuscript), showing the hourly mean evolution of atmospheric stability during the wet and dry seasons for both years analyzed. As shown in Figure S1, larger ζ = z/L values were associated with stronger atmospheric stability and shallower NBL, particularly during the dry season.

In addition, we expanded the analysis of the two case-study nights, including net radiation (Rn) at 81 m, cloud fraction (%), vertical profile of the potential temperature (θ) difference relative to 298 m, and vertical wind shear (dU/dz) for 18 and 25 August 2022 (Figure 4). To compute wind shear, third-order polynomial fits were applied to the wind speed profiles (U(z)), from which analytical vertical derivatives were calculated. Cloud fraction was estimated from observations obtained by the Cloud Radar Profiler (METEK MIRA-35C) installed at the ATTO site. GOES-16 IR Channel 13 (10.3 µm) brightness temperature imagery was additionally used to illustrate cloud cover conditions during the two nights (Figures 5 and 6).

The night of 18 August 2022 represents a strongly stratified and more decoupled case compared to 25 August 2022. Strong radiative cooling (Fig. 4a), reduced cloud occurrence (Fig. 4c and Fig. 5), and a pronounced vertical potential temperature gradient (Fig. 4e), were associated with a shallow hn, mostly around 80–100 m. Despite the presence of wind shear at some levels, the strong stratification suggests that mechanically generated turbulence aloft was not efficiently coupled downward to the layer near the canopy. This behavior is consistent with a layered nocturnal structure in which the shallow surface-based layer remains isolated from the air above, similar to the regime described by Mahrt and Acevedo (2023). In contrast, the night of 25 August 2022 showed larger cloud cover (Fig. 4d and Fig. 6), reduced radiative cooling during the early night (Fig. 4b), and weaker thermal stratification (Fig. 4f). Wind shear extended to higher levels (Fig. 4h), reaching approximately 150-170 m, close to hn. This suggests that mechanical forcing contributed to sustaining turbulence over a deeper layer under weaker stratification. Therefore, the differences between the two nights are interpreted as the result of the balance between radiative cooling, which enhances stratification and suppresses turbulence, and shear-generated mechanical turbulence, which can deepen or sustain the NBL when coupling is possible.

We included this new analysis in Section 3.3 of the Results and in the new Discussion section of the revised manuscript.

L239–253: To better identify the main drivers controlling the contrasting hn behavior during the two case-study nights, we further ana lyzed Rn at81m,cloudcover,the vertical profile of θ and windshear (dU/dz) (Fig. 9). These variables provide complementary information on the local radiative forcing, cloud modulation of nocturnal cooling, thermal stratification, and mechanical turbulence generation. The night of 18 August 2022 was characterized by strong nocturnal radiative cooling (Fig. 9a), reduced cloud occurrence (Fig. 9c and Fig. S2), and a pronounced vertical potential temperature gradient (Figure 9e). These conditions indicate enhanced thermal stratification near the surface. Although wind shear was observed at some levels (Fig. 9g), the strong stratification suggests that mechanically generated turbulence aloft was not efficiently coupled downward toward the canopy. This supports the interpretation that the shallow hn observed on 18 August 2022 reflects not only strong thermal stratification, but also canopy-induced suppression of vertical mixing near the forest top. This configuration is consistent with a shallow surface-based nocturnal layer that remained partly decoupled from the air above, similar to the layered nocturnal structure described by Mahrt and Acevedo (2023). In contrast, the night of 25 August 2022 showed larger cloud cover (Fig. 9d and Fig.S3), weaker radiative cooling during the early part of the night (Fig. 9b), and weaker thermal stratification (Fig. 9f). Wind shear extended to higher levels (Fig. 9h), reaching approximately 150–170 m, close to the observed hn. This suggests that, under weaker stratification, mechanically generated turbulence was more effectively coupled over a deeper layer, contributing to the larger and more variable hn observed during this night.

L289-322: The results presented here demonstrate that the nocturnal boundary-layer height (hn) above the central Amazon is strongly controlled by the interaction between nocturnal radiative cooling, atmospheric stability, cloud cover, and mechanically generated turbulence. Although previous Amazonian studies have primarily focused on the daytime evolution of the atmospheric boundary layer (Fisch et al., 2004; Carneiro and Fisch, 2020; Dias-Júnior et al., 2022), our results show that the nocturnal boundary layer also exhibits pronounced seasonal and interannual variability, with important implications for turbulence exchange and trace-gas transport above tropical forests.

One of the clearest patterns observed in this study is the systematic reduction of hn during the Dry season and during the El Niño year (2023). These periods were characterized by stronger nocturnal net radiative loss (Figure 2a) and enhanced atmospheric stability, reflected by larger z/L values (Figure 2b) and a stronger thermal gradient (Fig. S6b, d). Under these conditions, turbulent exchange becomes increasingly suppressed, limiting the upward transport of sensible heat and favoring the formation of shallower nocturnal layers (Figures 4d and 5b). In contrast, wetter conditions, particularly during the Wet season of 2022, were associated with weaker radiative cooling (Figure 2a), reduced stability (Figure 2b), Weak thermal gradient(Fig S6a, c), and deeper nocturnal layers (Figures 4a and 5a). These findings reinforce the strong coupling between cloud cover, nocturnal cooling, and turbulence generation over the Amazon rainforest.

The hourly evolution of hn also reveals the importance of the temporal evolution of thermal stratification during the night. In all analyzed periods, hn was generally larger at the beginning of the night and progressively decreased toward the early morning hours (Figure 5). This behavior is particularly evident during the Wet season of 2022, when the thermal gradient remained relatively weak during the first hours of the night (Figures 9e,f and S6a), allowing mechanically generated turbulence to sustain a deeper nocturnal boundary layer. As the night progressed, radiative cooling intensified the thermal gradients, suppressing turbulence and leading to a gradual collapse of hn. This progressive reduction of turbulent mixing throughout the night is consistent with the classical evolution of stable nocturnal boundary layers described in previous studies (Mahrt, 1999; Sun et al., 2002).

The results also demonstrate that the interaction between thermal stratification and mechanically generated turbulence is fundamental for understanding the nocturnal boundary-layer structure above the Amazon forest (Figure 9). The case studies revealed that low-level jets (LLJs) (Figure 7) and enhanced vertical wind shear (Figure 9 g,h) may sustain turbulence above the canopy, but the influence of this turbulence on the lower nocturnal boundary layer depends on the degree of vertical coupling between atmospheric layers. This interpretation is consistent with the conceptual framework proposed by Mahrt and Acevedo (2023), in which nocturnal boundary layers may deviate from a vertically monotonic structure and instead exhibit layered configurations composed of shallow surface-based layers, transition layers, and elevated turbulent regions.

Our observations suggest that the forest canopy plays a key role in reinforcing this layered structure. Under strongly stable conditions, the canopy acts as a roughness and drag layer that attenuates momentum transfer toward the surface. Consequently, turbulence generated aloft by LLJs or strong wind shear may remain confined to elevated layers and may not efficiently penetrate downward through the canopy layer. This mechanism likely explains the shallow hn observed on 18 August 2022, when strong thermal stratification and weak vertical coupling produced a highly decoupled nocturnal structure. In contrast, on 25 August 2022, weaker thermal stratification allowed mechanically generated turbulence to penetrate deeper into the lower nocturnal boundary layer, resulting in larger and more vertically connected hn values.

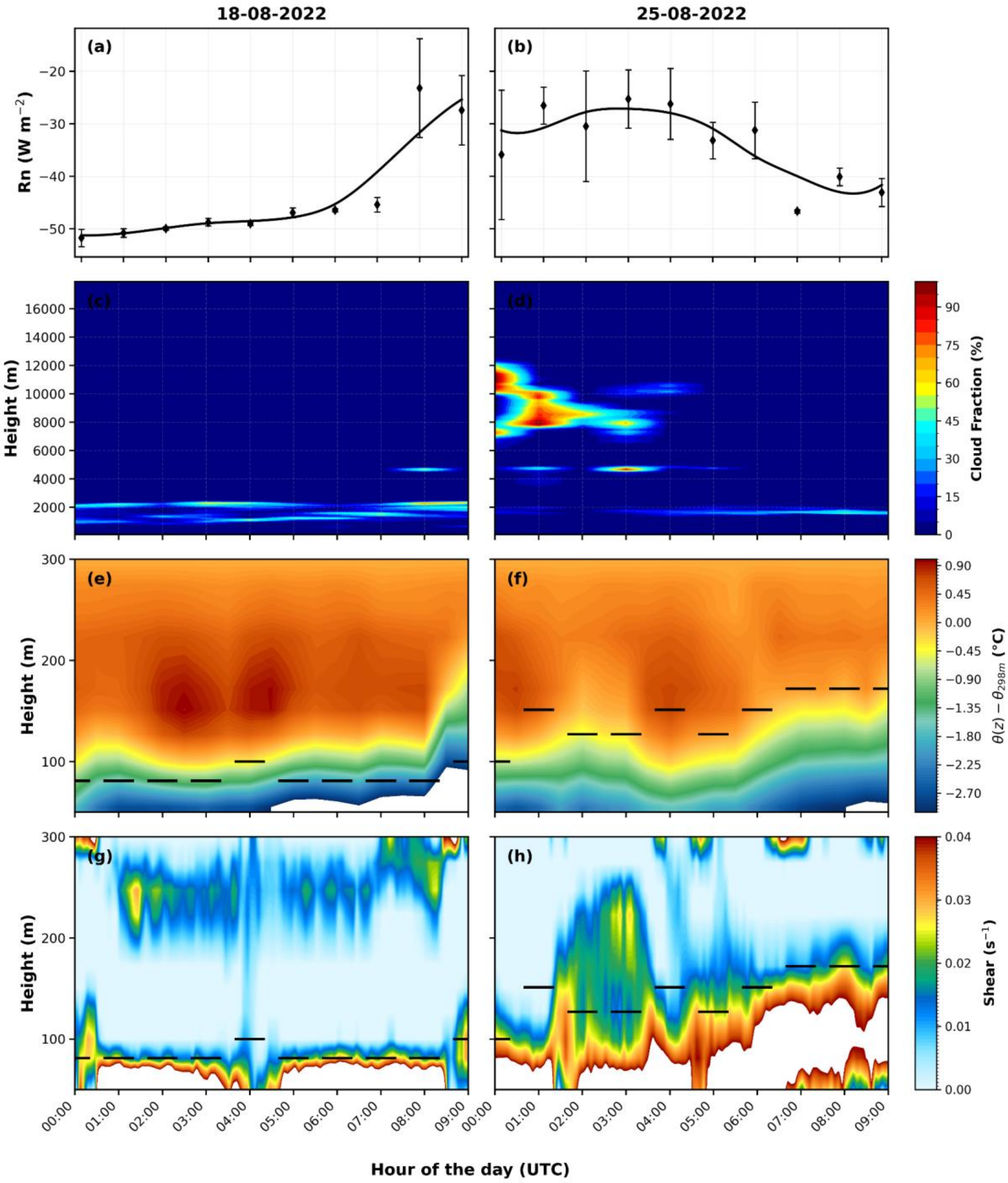

Figure 4 (Figure 9 in new version of the manuscript). Nocturnal evolution of (a, b) hourly mean net radiation (Rn) at 81 m (± standard deviation), (c, d) cloud fraction (%), (e, f) vertical potential temperature (θ) difference from the value observed at 298 m, and (g, h) vertical wind shear (dU/dz) during the case-study nights of 18 August 2022 (left panels) and 25 August 2022 (right panels). Black horizontal segments indicate the estimated nocturnal boundary layer height at each hour.

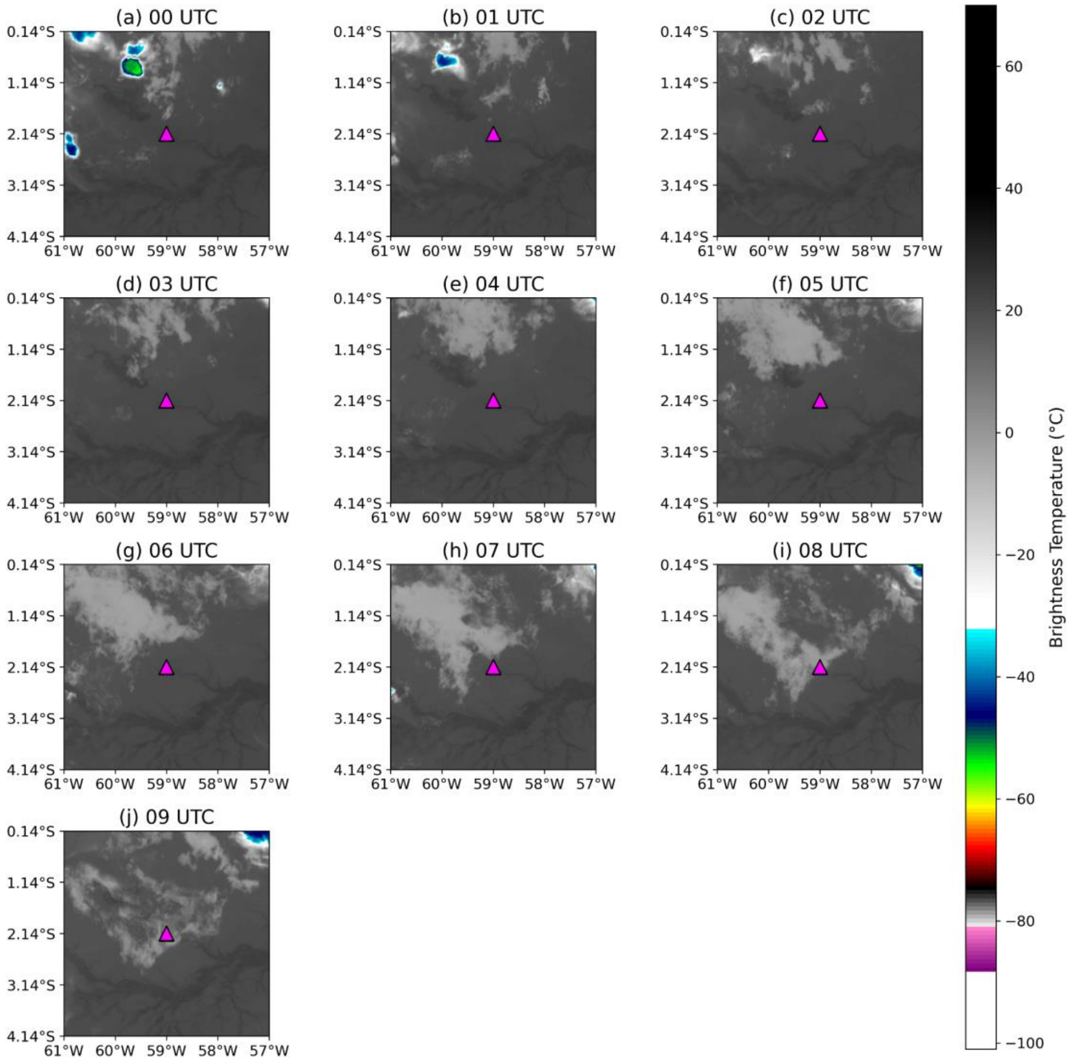

Figure 5 (Figure S2 in new version of the manuscript). GOES-16 IR Channel 13 (10.3 µm) brightness temperature over the ATTO site on 18 August 2022. Panels (a–j) show hourly images from 00 to 09 UTC. The magenta triangle marks the location of the ATTO tower.

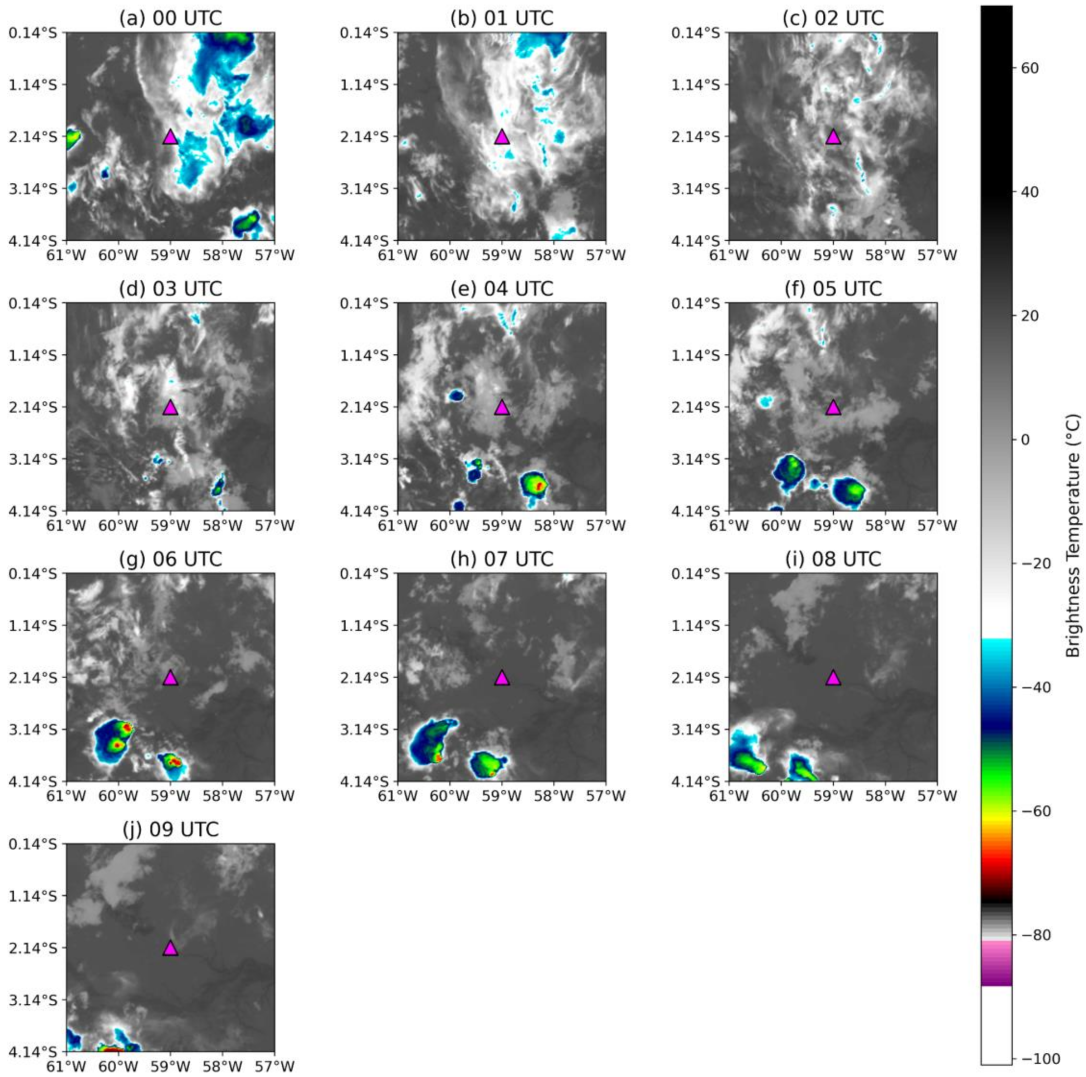

Figure 6 (Figure S3 in new version of the manuscript). GOES-16 IR Channel 13 (10.3 µm) brightness temperature over the ATTO site on 25 August 2022. Panels (a–j) show hourly images from 00 to 09 UTC. The magenta triangle marks the location of the ATTO tower.

• Lines 178-184: The authors attribute the differences in nocturnal radiative loss and boundary-layer structure primarily to variations in cloud cover (e.g., "greater cloud cover results in greater turbulent activity"). While this mechanism is physically plausible from a boundary-layer meteorology perspective, the manuscript does not present a direct metric of cloud cover to support this interpretation. The analysis appears to rely on radiation measurements (e.g., net radiation, Rn), which can indeed reflect differences in radiative cooling but do not uniquely indicate cloudiness. I therefore suggest that the authors either (i) provide additional evidence linking the radiation differences to cloud cover (e.g., through analysis of longwave radiation or another proxy for cloudiness), or (ii) rephrase the discussion more cautiously, framing cloud cover as one possible explanation for the observed radiative differences rather than a demonstrated cause.

We thank Reviewer #2 for this comment. We expanded the analysis of the two case-study nights, as described in the response to the previous comment (Line 224-333 in this document).

These additional observations indicate lower (higher) cloud occurrence on 18 August 2022 (25 August 2022), consistent with the observed differences in net radiation between the two cases.

We added this discussion to Section 3.3 of the revised manuscript (L239-253).

L239–253: To better identify the main drivers controlling the contrasting hn behavior during the two case-study nights, we further ana lyzed Rn at81m,cloudcover,the vertical profile of θ and windshear (dU/dz) (Fig. 9). These variables provide complementary information on the local radiative forcing, cloud modulation of nocturnal cooling, thermal stratification, and mechanical turbulence generation. The night of 18 August 2022 was characterized by strong nocturnal radiative cooling (Fig. 9a), reduced cloud occurrence (Fig. 9c and Fig. S2), and a pronounced vertical potential temperature gradient (Figure 9e). These conditions indicate enhanced thermal stratification near the surface. Although wind shear was observed at some levels (Fig. 9g), the strong stratification suggests that mechanically generated turbulence aloft was not efficiently coupled downward toward the canopy. This supports the interpretation that the shallow hn observed on 18 August 2022 reflects not only strong thermal stratification, but also canopy-induced suppression of vertical mixing near the forest top. This configuration is consistent with a shallow surface-based nocturnal layer that remained partly decoupled from the air above, similar to the layered nocturnal structure described by Mahrt and Acevedo (2023). In contrast, the night of 25 August 2022 showed larger cloud cover (Fig. 9d and Fig.S3), weaker radiative cooling during the early part of the night (Fig. 9b), and weaker thermal stratification (Fig. 9f). Wind shear extended to higher levels (Fig. 9h), reaching approximately 150–170 m, close to the observed hn. This suggests that, under weaker stratification, mechanically generated turbulence was more effectively coupled over a deeper layer, contributing to the larger and more variable hn observed during this night.

• Line 185: Mention briefly these methods

This clarification has been incorporated into the new discussion section of the revised manuscript as follows:

L345-347: “Most previous studies relied on indirect methods based on thermodynamic profiles, Richardson number, or remote sensing approaches (Santos et al., 2007; Dias-Júnior et al., 2022; Carneiro et al., 2025). ”

• Line 186: Based on which method ?

Mendonça et al. (2025) used the same dataset and methodology adopted in this study, as detailed in response to a previous comment (Line 81 in this document). The text has been updated to improve clarity:

L60-61: “These estimates are based on the height at which H falls below 5% of its near-surface value ”

L347-349: More recently, Mendonça et al. (2025) used the same turbulence-based methodology and reported hn values ranging between approximately 81 and 223 m, demonstrating the importance of surface roughness and topography for nocturnal boundary-layer structure

• Figure 8 does not differentiate between the 2 selected dates (add respectively in the caption) .

We thank the reviewer for this suggestion. Figure 8 has been revised to include the respective dates in the figure titles and captions.

References:

Carneiro, R., Fisch, G., Neves, T., Santos, R., Santos, C., and Borges, C.: Nocturnal boundary layer erosion analysis in the Amazon using large-eddy simulation during GoAmazon project 2014/5, Atmosphere, 12, 240, 2021

Dias-Júnior, C. Q., Carneiro, R. G., Fisch, G., D'Oliveira, F. A. F., Sörgel, M., Botía, S., Machado, L. A. T., Wolff, S., Santos, R. M. N. d., and Pöhlker, C.: Intercomparison of planetary boundary layer heights using remote sensing retrievals and ERA5 reanalysis over Central Amazonia, Remote Sensing, 14, 4561, 2022.

Dias, N. L., Toro, I. M. C., Dias-Júnior, C. Q., Mortarini, L., and Brondani, D.: The relaxed eddy accumulation method over the amazon forest: the importance of flux strength on individual and aggregated flux estimates, Boundary-Layer Meteorology, 189, 139–161, 2023.

Fisch, G., Tota, J., Machado, L., Silva Dias, M. A. F. d., Da F. Lyra, R., Nobre, C., Dolman, A., and Gash, J.: The convective boundary layer over pasture and forest in Amazonia, Theoretical and Applied Climatology, 78, 47–59, 2004

Foken, T., & Mauder, M. (2008). *Micrometeorology* (Vol. 2, p. 306). Berlin: Springer.

Huitema, A. C., de Feiter, V. S., González-Armas, R., Hartogensis, O. K., van Asperen, H., Quaresma Dias-Júnior, C., & Vilà-Guerau de Arellano, J. (2026). CO 2 and Heat exchange across the Nocturnal Canopy–Atmosphere interface in the Amazon rainforest. *EGUsphere*, *2026*, 1-32.

Kaimal, Jagadish Chandran; FINNIGAN, John J. Atmospheric boundary layer flows: their structure and measurement. Oxford university press, 1994.

Lenschow, D. H., Li, X. S., Zhu, C. J., and Stankov, B. B.: The stably stratified boundary layer over the Great Plains: I. Mean and turbulence structure, Boundary-layer meteorology, 42, 95–121, 1988

Mendonça, A. C., Dias-Junior, C. Q., Acevedo, O. C., Marra, D. M., Cely-Toro, I. M., Fisch, G., Brondani, D. V., Manzi, A. O., Portela, B. T., Quesada, C. A., et al.: Estimation of the nocturnal boundary layer height over the Central Amazon forest using turbulence measurements, Agricultural and Forest Meteorology, 367, 110469, 2025

Nieuwstadt, Frans TM. The turbulent structure of the stable, nocturnal boundary layer. Journal of Atmospheric Sciences, v. 41, n. 14, p. 2202-2216, 1984.

Oliveira, P. E., Acevedo, O. C., Sörgel, M., Tsokankunku, A., Wolff, S., Araújo, A. C., ... & Andreae, M. O. (2018). Nighttime wind and scalar variability within and above an Amazonian canopy. *Atmospheric Chemistry and Physics*, *18*(5), 3083-3099.

Starkenburg, D., Metzger, S., Fochesatto, G. J., Alfieri, J. G., Gens, R., Prakash, A., and Cristóbal, J.: Assessment of despiking methods for turbulence data in micrometeorology, Journal of Atmospheric and Oceanic Technology, 33, 2001–2013, 2016

Stull, R. B. (1988). Mean boundary layer characteristics. In *An introduction to boundary layer meteorology* (pp. 1-27). Dordrecht: Springer Netherlands.

Sun, J., Burns, S. P., Lenschow, D. H., Banta, R., Newsom, R., Coulter, R., ... & Hu, X. Z. (2002). Intermittent turbulence associated with a density current passage in the stable boundary layer. *Boundary-Layer Meteorology*, *105*(2), 199-219.

Vickers, D. and Mahrt, L.: Quality control and flux sampling problems for tower and aircraft data, Journal of atmospheric and oceanic technology, 14, 512–526, 1997

Vickers, D., & Mahrt, L. (2004). Evaluating formulations of stable boundary layer height. *Journal of applied meteorology*, *43*(11), 1736-1749.

Wilczak, J. M., Oncley, S. P., & Stage, S. A. (2001). Sonic anemometer tilt correction algorithms. *Boundary-layer meteorology*, *99*(1), 127-150.

Zahn, E., Chor, T., and Dias, N.: A simple methodology for quality control of micrometeorological datasets, Am J Environ Eng, 6, 135–142, 2016